MICROMECHANICAL MODELLING OF NON-HOMOGENOUS MATERIALS BY MESHLESS METHODS

N.Muthu[1] , B.G. Falzon[2] , S.K. Maiti[3] and W. Yan[4]

[1]IITB-Monash Research Academy,
IIT Bombay, Mumbai, 400076, India
Email: mnelson1986@gmail.com, web page: http://www.iitbmonash.org/

[2]Department of Mechanical and Aerospace Engineering,
Queen's University, Belfast, UK
Email: b.falzon@qub.ac.uk, web page: https://www.qub.ac.uk

[3]Department of Mechanical Engineering,
IIT Bombay, Mumbai, 400076, India
Email: skmaiti@iitb.ac.in, web page: http://www.iitb.ac.in/

[4]Department of Mechanical and Aerospace Engineering,
Monash University, Clayton,
VIC 3800, Australia
Email: wenyi.yan@monash.edu, web page: http://www.monash.edu/

Keywords: Meshless methods, Crack propagation, Functionally graded materials, Bi-material interface, Fiber-matrix composite

ABSTRACT

A detailed study of bi-material composites, using meshless methods (MMs), is presented in this paper. Firstly, representative volume elements (RVEs) for different bi-material combinations are analysed by the element-free Galerkin (EFG) method in order to confirm the effective properties of heterogeneous material through homogenization. The results are shown to be in good agreement with experimental results and those obtained using the finite element method (FEM) which required a higher node density. Secondly, a functionally graded material (FGM), with a crack, is analysed using the EFG method. This investigation was motivated by the possibility of replacing the distinct fibre-matrix interface with a FGM interface. Finally, an illustrative example showing crack propagation, in a two-dimension micro-scale model of a SiC/Al composite is presented.

1 INTRODUCTION

This paper explores the use of meshless methods (MMs) to characterise the fracture of non-homogenous materials. Although the finite element method (FEM) is used extensively to model crack propagation in composite materials, it presents some challenges if re-meshing is required as the crack propagates. To overcome the difficulties associated with meshing, MMs and the eXtended finite element method (XFEM) [1] were developed. Modelling crack growth, in non-homogenous materials, using the partition-of-unity approach XFEM is difficult because the enrichment functions change, depending on the material under investigation, location of the crack tip and the type of loading [2]. In general, the shape functions of the MMs are of higher continuous order than the shape functions of FEM or XFEM. Therefore, a relatively courser nodal discretization is sufficient to model fracture using the element-free Galerkin (EFG) meshless method [3].

Crack propagation in non-homogenous materials involves an order of stress singularity other than $r^{-0.5}$ where r is the radial distance from the crack tip. The order of singularity is $r^{-0.5}$, if the tip is

embedded inside the homogenous medium and $\sigma_{ij} \propto r^{\lambda-1}$ at a bi-material interface. λ can be real single, double ($0 < \lambda < 1$) or complex depending on the material combination and angle made by the crack with the interface [4].

In general, the fibre-matrix interface is of finite thickness, whose dimension varies depending on the material combination and manufacturing process. A crack in a distinct interface may be unrealistic and increases the computational effort. In this work, the possibility of replacing this discontinuity with a FGM interface is examined.

2 EFG METHOD

In the displacement-based EFG method, the displacement at location $\mathbf{x}$, within a support domain of n nodes, $\mathbf{u}(\mathbf{x})$, can be represented as

$$\mathbf{u}(\mathbf{x}) = \sum_{I=1}^{n} \Phi_I(\mathbf{x})\mathbf{u}_I \tag{1}$$

where $\Phi_I(\mathbf{x})$ are the nodal shape functions and $\mathbf{u}_I$ are the nodal displacement vectors. The moving least squares (MLS) interpolation technique is used to develop the shape functions in the EFG method.

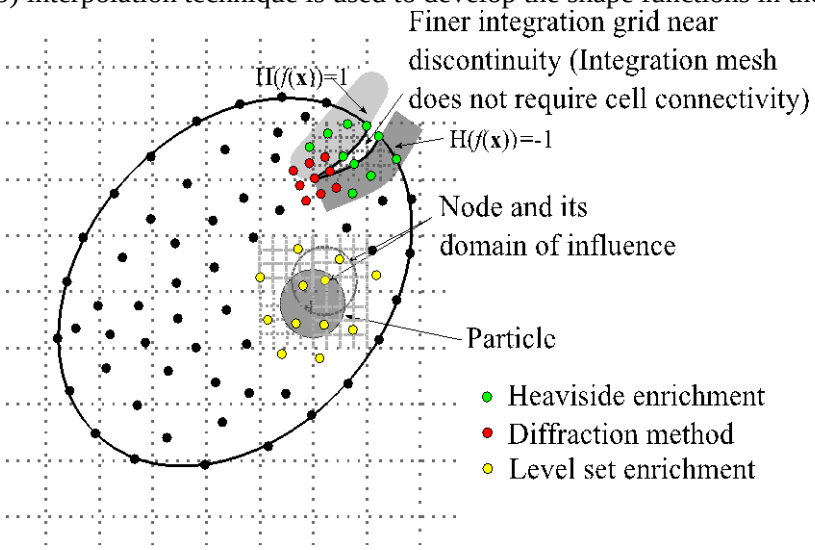

Figure 1: Nodal discretization for a domain with a crack and an inclusion.

In this work, the Heaviside function is used to take care of the discontinuity between the crack edges and the diffraction method is used in the region around the crack tip. The diffraction method eliminates the need of enrichment functions that depend on the location of the crack tip, orientation of the crack to a material interface and material properties. The Heaviside function helps to avoid the need of adding additional nodes along the crack faces in a problem of mixed-mode crack propagation. Consequently, the displacement approximation in the proposed EFG method in the presence of a crack (strong discontinuity) and inclusion boundary (weak discontinuity) present in a given geometry (Figure 1), takes the form

$$\mathbf{u}(\mathbf{x}) = \sum_{I \in w(\mathbf{x})} \Phi_I(\mathbf{x})\mathbf{u}_I + \sum_{I \in w_j(\mathbf{x})} \Phi_I(\mathbf{x})\{\mathbf{a}_I \mathrm{H}(f(\mathbf{x}))\} + \sum_{I \in w_c(\mathbf{x})} \Phi_I(\mathbf{x})\mathbf{c}_I \chi_I(\mathbf{x}) \tag{2}$$

where function $\chi_I(\mathbf{x}) = \mathrm{F}^I(\mathbf{x}) - \mathrm{F}^I(\mathbf{x}_I)$ is employed for displacement continuity across the interface with $\mathrm{F}^I(\mathbf{x}) = \sum_{I \in w_c(\mathrm{x})} |\zeta_I| \Phi_I(\mathbf{x}) - \left| \sum_{I \in w_c(\mathrm{x})} \zeta_I \Phi_I(\mathbf{x}) \right|$. ζ_I is the signed distance of node *I* from the interface [5].

The set $w(\mathbf{x})$ consists of nodes in the support domain of $\mathbf{x}$. The set $w_j(\mathbf{x})$ and $w_c(\mathbf{x})$ consist of Heaviside and level set enriched nodes, respectively.

The routinely used polynomial basis $\mathrm{p}=[1 \; x \; y]$ needed for the development of the shape functions for the EFG method, through the MLS technique, is employed. The cubic B-spline weight function with a circular domain of influence is used.

3 HOMOGENIZATION APPROACH

Homogenization is often utilised to assign a composite material with the volume-averaged mechanical properties of a representative volume element (RVE). The average stresses and strains in a RVE are defined by

$$\varepsilon_{ij}^0 = \frac{\int_V \varepsilon_{ij} dV}{V} \qquad \sigma_{ij}^0 = \frac{\int_V \sigma_{ij} dV}{V} \tag{3}$$

where, within the context of MMs, σ_{ij} and ε_{ij} are the numerical stress and strain computed at each Gauss point of the background mesh. V is the volume of the RVE.

The effective properties C_{ijkl} of a composite can then be obtained using

$$C_{ijkl} = \frac{\sigma_{ij}^0}{\varepsilon_{kl}^0} \tag{4}$$

Three types of boundary conditions can be prescribed on an individual volume element in order to compute the C_{ijkl} tensor. They are:

1. Homogenous boundary conditions [6].
2. Periodic boundary conditions [7].
3. Prescribed displacement boundary conditions [8].

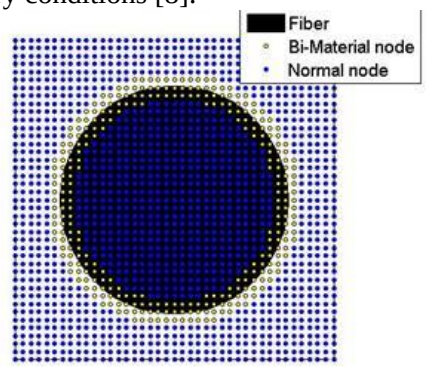

Figure 2: Nodal discretization of 2D RVE.

In this work, prescribed displacement boundary conditions are used. The application of this boundary condition can guarantee the displacement continuity and traction continuity at the boundaries of the RVE which can mimic the solution for real periodic structure [8]. Moreover, this is simple to prescribe on the boundaries of a RVE. A typical 2D RVE with nodal discretisation including the bi-material nodes is shown in Figure 2.

To calculate the Young's modulus and Poisson's ratio, the following displacements are prescribed: U_{right} =0.05; V_{top}=V_{bottom}=0; U_{left} =0. To calculate the shear modulus, the following displacements are prescribed: V_{right} =0.05, V_{left} =-0.05; U_{top}=0.05, U_{bottom}=-0.05; $U_{left,bottom}$ =$V_{left,bottom}$=0.

4 STRESS INTENSITY FACTOR AND CRACK PROPAGATION CRITERIA

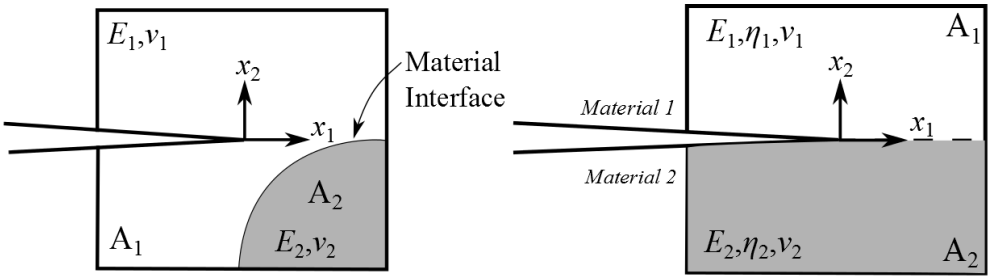

(a) (b)

Figure 3: Domain of integration **(a)** consisting of material interfaces; **(b)** for interface crack.

Mixed mode SIFs can be computed through the interaction integral/M-integral [9] within the framework of MMs. For a crack in a homogenous material, in the presence of material interfaces, the interaction integral is given by

$$I = \int_A (\sigma_{ij} u_{i,1}^{aux} + \sigma_{ij}^{aux} u_{i,1} - \sigma_{ik} \varepsilon_{ik}^{aux} \delta_{1j}) q_{,j} dA + \int_A \sigma_{ij} \{S_{ijkl}^{tip} - S_{ijkl}(\mathbf{x})\} \sigma_{kl,1}^{aux} q dA \tag{5}$$

where $A = A_1 + A_2$ is the area of integration as shown in Figure 3(a). q is a scalar function; it has the value of unity at the crack tip and zero on the boundary of the integral domain. $S_{ijkl}(\mathbf{x})$ and S_{ijkl}^{tip} are entries in the compliance matrix at any point $\mathbf{x}$ inside the domain and the crack tip respectively. σ_{ij}^{aux}, ε_{ik}^{aux} and u_i^{aux} are auxiliary state values that correspond to the theoretical crack tip solution in a homogenous material.

For a crack in an isotropic and homogenous material, the interaction integral/M-integral is equal to

$$I = \frac{(2K_I K_I^{aux} + 2K_{II} K_{II}^{aux})}{E^*} \tag{6}$$

where E^* is E for plane stress and $E/(1\text{-}\nu^2)$ for plane strain. E and ν are, respectively, Young's modulus and Poisson's ratio. K_I is evaluated by setting K_I^{aux} to unity and K_{II}^{aux} to zero. Similarly K_{II} is evaluated by setting K_{II}^{aux} to unity and K_I^{aux} to zero.

In case of an interface crack in bi-materials, as shown in Figure 3(b), subjected to mechanical and thermal load, ΔT, the interaction integral [10] is given by

$$I = \sum_{m=1}^{2} \int_{A_m} (\sigma_{ij} u_{i,1}^{aux} + \sigma_{ij}^{aux} u_{i,1} - \sigma_{ik} \varepsilon_{ik}^{aux} \delta_{1j}) q_{,j} dA + \sum_{m=1}^{2} \varphi_m \int_{A_m} \varepsilon_{kk}^{aux} (\Delta T)_{,1} q dA \tag{7}$$

$$\varphi = \begin{matrix} E\eta/(1-2\nu) \ for\ plane\ strain \\ E\eta/(1-\nu) \ for\ plane\ stress \end{matrix}$$

η is the thermal coefficient of the material. σ_{ij}^{aux}, ε_{ik}^{aux} and u_i^{aux} are crack tip solution for an auxiliary state with an interface crack. The SIFs can be computed using the following relation,

$$I = \frac{(1/E_1^* + 1/E_2^*)(2K_I K_I^{aux} + 2K_{II} K_{II}^{aux})}{2\cosh^2(\pi\varepsilon)} \tag{8}$$

ε is an oscillatory parameter for bi-materials. For a bi-material consisting of two isotropic materials, it is defined as

$$\varepsilon = \frac{1}{2\pi}\ln\left(\frac{\kappa_1\mu_2 + \mu_1}{\kappa_2\mu_1 + \mu_2}\right) \tag{9}$$

where μ is the shear modulus and κ is the Kolosov constant. Usually, the SIFs can be extracted using a square integral domain with edge length ranging from $0.125a$ to $0.25a$ where a is the crack length.

4.1 Crack propagation criteria

The stress state for an interface crack of length, a, is given by

$$\sigma_{ij}^m = \frac{F_{ij}^m(\theta)}{\sqrt{r}}\mathrm{Re}\left[\mathbf{K}r^{i\varepsilon}\right] + \frac{G_{ij}^m(\theta)}{\sqrt{r}}\mathrm{Im}\left[\mathbf{K}r^{i\varepsilon}\right] + T_m\delta_{i1}\delta_{j1} + O(\sqrt{r}) \tag{10}$$

where $\mathbf{K} = K_1 + iK_2$ (complex SIF) and T_m is the T-stress for material m. The angular functions $F_{ij}^m(\theta)$ and $G_{ij}^m(\theta)$ are given in [11]. The stresses, σ_{22} and σ_{12}, at the interface in front of the crack tip as shown in Figure 4(a), for $\theta = 0$, are given by

$$\boldsymbol{\sigma} = (\sigma_{22} + i\sigma_{12})_{\theta=0} = \frac{K_1 + iK_2}{\sqrt{2\pi r}}r^{i\varepsilon} \tag{11}$$

It has been pointed out that the T-stress, which is parallel to the interface, affects the behavior of the crack kinking out of the interface [12]. This is taken into account in determining the kinking angle, ω, as shown in Figure 4(b).

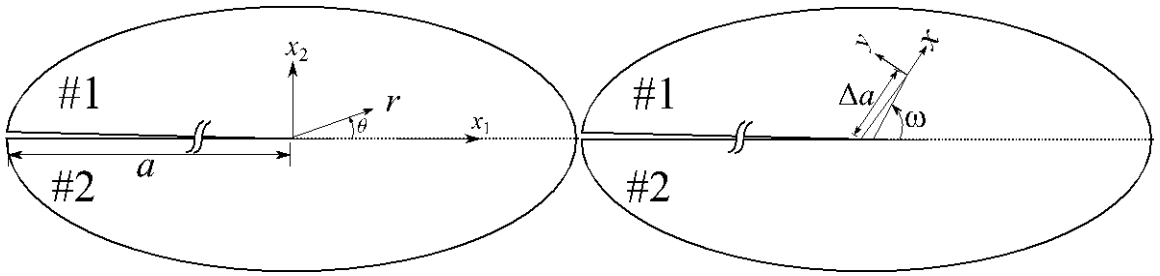

Figure 4: **(a)** Interface Crack **(b)** Kinking of an interface crack.

There are three criteria which are widely reported in the literature to determine ω; (a) $G_{\max}$ criterion [13] based on the maximum energy release rate. (b) $\sigma_{\theta\theta}^{\max}$ criterion [14] based on the maximum hoop stress given in terms of the SIFs, and (c) $K_{II} = 0$ criterion [15] for a kinked crack of length Δa.

The $G_{\max}$ criterion requires multiple analyses, within the framework of MMs, to determine the kinking angle; the $\sigma_{\theta\theta}^{\max}$ criterion, by itself and without knowledge of the energy release rate, cannot determine whether the crack will propagate at a determined kink angle. The zero K_{II} criterion is based on mixed mode SIFs of kinked crack of length, Δa. It assumes that the crack will kink in the direction of the zero mode II SIF ($K_{II} = 0$) or pure mode I of the kinked crack. Similar to $G_{\max}$ criterion, this criterion too needs multiple analyses as one needs to test the kinked crack in various directions to find the pure mode I direction.

In this work, during crack propagation, a criterion based on both the stress state and energy release rate conditions are used to predict the kinking angle and its onset. While the stress criterion gives the direction of crack propagation, the energy criterion ascertains whether the crack propgates. The crack initiates when the energy release rate (G) exceeds the critical energy release rate (G_c).

The necessary condition for a crack kinking at an angle ω is that the shear stress, $\tau_{r\theta}$, obtained from the SIFs and T-stress, goes to zero. This is based on Rankine's theory that assumes that the failure will occur at an angle when the maximum tangential principal stress (MTPS) ($\sigma_{\theta P}$) reaches the tensile strength of the material. Such a criterion as shown in Figure 5, known as MTPS criterion, has been found suitable for determining the kinking angle for a crack in homogenous and isotropic materials [16].

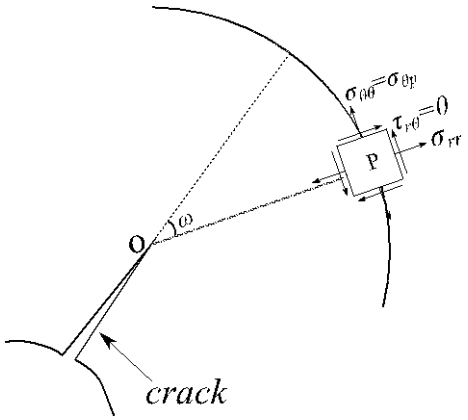

Figure 5**:** Kinking angle based on zero shear stress criterion.

The stress field in the region close to the crack tip is determined using SIFs and T-stress obtained from the interaction integral. The T-stress can be obtained by selecting the appropriate auxiliary stresses (σ_{ij}^{aux}), strains (ε_{ik}^{aux}) and displacements (u_i^{aux}) in the interaction integral (Appendix A). The T-stress is related to the interaction integral by

$$T_m = \frac{IE_m^*}{f} \tag{12}$$

where T_m is the T-stress in the material m (m=1, 2) and f is a point unit force applied. The auxiliary field corresponds to this force.

The sufficient condition for an interface crack to kink at an angle, ω, is given by

$$\frac{G_{m\omega}}{\Gamma_f^m} > \frac{G_I}{\Gamma_f^I} \tag{13}$$

where Γ_f^m and Γ_f^I are the fracture toughness of the adjoining material and the interface. The ERR (G_I) along the interface and ERR ($G_{m\omega}$) along the kinking angle, ω, are given by the following relations.

$$\begin{aligned} G_I &= \frac{1}{E^*}\frac{K_1^2+K_2^2}{\cosh^2(\pi\varepsilon)} \\ G_{m\omega} &= \frac{1}{E_m^*}\frac{K_I^2+K_{II}^2}{2} \\ 1/E^* &= 1/E_1^* + 1/E_2^* \end{aligned} \tag{14}$$

The crack is likely to penetrate into the homogenous neighbouring material if the inequality in eq. (13) holds. Otherwise, it is likely to extend along the interface.

5 CASE STUDIES

4.1 Meshfree analysis of a 2D RVE

Three-square 2D RVEs of different material combinations were analyzed using the proposed EFG method. Table 1 consists of elastic constants of various fibre and matrix materials. Prescribed displacement boundary conditions were imposed on the RVE to obtain effective Young's and shear moduli. Figure 6 and Figure 7 show comparisons with Hashin-Shtrikman's variational bounds for macroscopically isotropic composites [17] and experimental values [18, 19].

Table 1: Elastic constants for various materials.

Fiber Material	Fiber		Matrix Material	Matrix	
	E (GPa)	ν		E (GPa)	ν
Glass	43.1	0.22	Epoxy	3.45	0.35
SiC	419.4	0.16	Al	76.8	0.33
Carbon	15	0.49	Epoxy	3.45	0.35

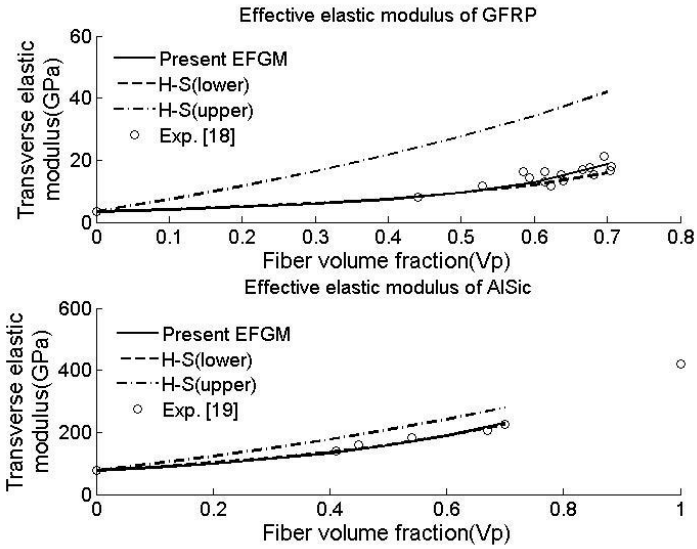

Figure 6: Comparison between predicted and measured value of transverse Young's modulus of glass-epoxy and Al/SiC composite.

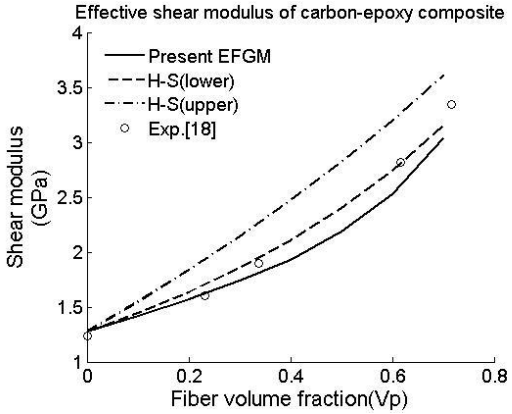

Figure 7: Comparison between predicted and measured value of shear modulus of carbon-epoxy composite.

Figure 6 and Figure 7 show that the computed results are in good agreement with the published experimental results.

4.2 Mode I crack in a functionally graded material

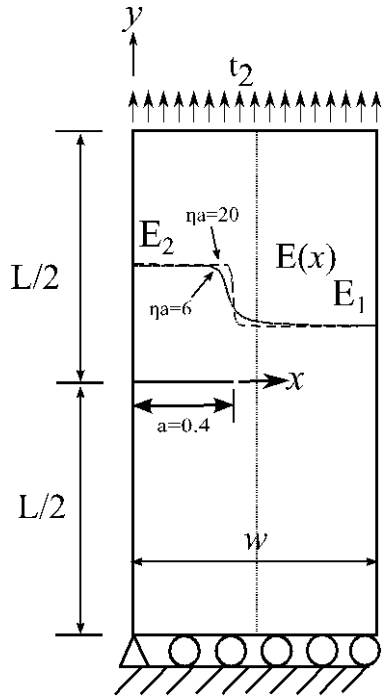

Figure 8: Composite strip with a mode I edge crack.

A composite strip with a mode I edge crack ($a/w = 0.4$), as shown in Figure 8, has dimensions, $w = 1\,\text{m}$ (width) and $L/w = 2$ (length-to-width). The Poisson's ratio ν was kept constant with a value of 0.3. The Young's modulus is a function of the hyperbolic tangent function, given by

$$E(\text{x}) = \frac{E_1 + E_2}{2} + \frac{E_1 - E_2}{2}\text{Tanh}(\eta(x - 0.4)) \tag{15}$$

where $E_1 = 1\text{GPa}$ and $E_2 / E_1 = 3$. The rate of change of material properties at the crack tip increases as η increases. A tensile traction of $\text{t}_2 = \bar{\varepsilon}E(x)/(1-\nu^2)$, where $\bar{\varepsilon}$ = 0.001, was applied on the upper boundary of the composite strip to ensure uniform strain. A plane strain condition was assumed. The composite was discretized with 21×41 nodes and the domain of influence was set at 1.75 times the nodal spacing.

Table 2: Normalized mode I SIF for composite strip.

ηa	Normalized SIF		% difference
	Ref. [20]	EFG method	
0	2.112	2.042	3.32%
2	2.295	2.218	3.35%
4	2.571	2.484	3.39%
6	2.733	2.640	3.42%
20	3.228	3.094	4.14%

Table 2 shows the mode I SIFs obtained for different values of ηa. The normalized SIF results were normalized ($(1-\nu^2)K_I / \bar{\varepsilon}E(x=0)\sqrt{\pi a}$) and compared with published results (Table 2) obtained using

the XEFG method through crack closure integral approach to extract SIFs. The mode I SIFs obtained by the interaction integral method are in good agreement with those in the literature (which used enrichment functions and the crack closure integral) with an average difference of 3.52%.

4.3 Fibre-matrix interface of finite thickness

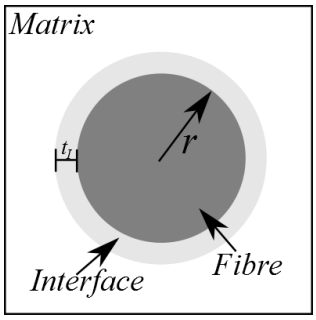

Figure 9: Fibre-matrix interface with thickness t_I.

An RVE with fibre-matrix interface of finite thickness t_I (Figure 9) was subjected to prescribed displacement boundary conditions to compute the variation of homogenized material properties with t_I. Figure 10 shows the variation of error in transverse Young's modulus of GFRP RVE, of volume fraction ($V_P = 0.44$), and Al/SiC RVE, of volume fraction ($V_P = 0.41$), with t_I. The % error is obtained by comparing the results with experimental results GFRP ($V_P = 0.44$): E=8.24GPa [18], AlSiC ($V_P = 0.41$): E=139GPa [19]. The Young's modulus and Poisson's ratio variation in the interface region were assumed to be

$$E(x) = \frac{E_f + E_m}{2} + \frac{E_m - E_f}{2}\mathrm{Tanh}(\eta(r - r_f))$$
$$\nu(x) = \frac{\nu_f + \nu_m}{2} + \frac{\nu_m - \nu_f}{2}\mathrm{Tanh}(\eta(r - r_f)) \quad (16)$$

where E_m and E_f are the Young's modulus of matrix and fibre respectively. ν_m and ν_f are the Poisson's ratio of matrix and fibre respectively.

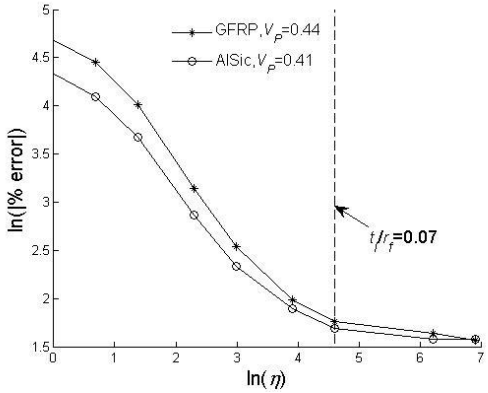

Figure 10: Variation of error in transverse Young's modulus with parameter η.

Figure 10 shows that $\eta \geq 100(\ln(\eta) \geq 4.6)$ reduces the % error in transverse Young's modulus less than 5%. This η corresponds to $t_I / r_f \approx 0.07$. In other words, the thickness of the interface

could be restricted within $0.07r_f$ to obtain satisfactory results. For practical purposes, $0.04r_f \le t_I \le 0.07r_f$, so that the interface effects are captured by the EFG method without the need for higher nodal discretization while ensuring good results.

4.4 Crack propagation in non-homogenous materials

A starter crack of $2a/L$ = 0.4 at d/L = 0.05 and $2a/L$ = 0.65 at d/L of -0.205 were investigated separately in a square plate of side $L=2\,\mathrm{m}$. The particles are of radius, $2r/L = 0.18$ and distributed as shown in Figure 11(a). The plate was subjected to a uniform tension of $\sigma = 1\mathrm{MPa}$. A plane strain condition was assumed. The particle material modulus was $E_p = 6.43E_m$. The particle and matrix Poisson's ratio were: $v_p = 0.17$ and $v_m = 0.33$. These values correspond to silicon carbide (SiC) particle reinforcement in aluminum (Al) matrix.

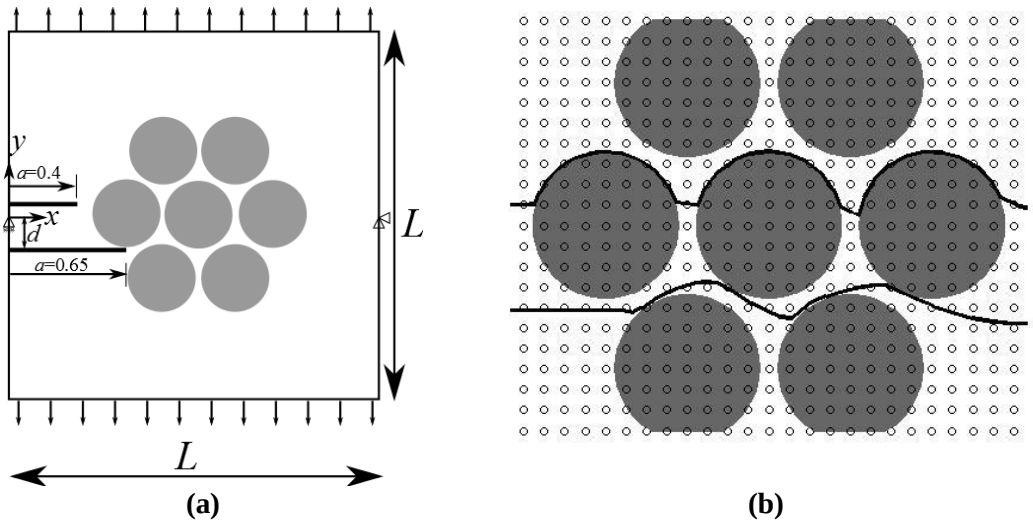

Figure 11: **(a)** Composite strip with a mode I edge crack; **(b)** Crack path.

The crack path propagated along the interface of the three particles as shown in Figure 11(b) for the starter crack at $2a/L$ = 0.4. This crack propagates as an interface crack for a while before entering the matrix. The conditions for the crack deviating from the interface depend on the fracture toughness of the interface as well as the aluminium matrix. In the second example, the crack is deflected by the SiC particles to a lesser extent and propagates primarily within the matrix. The nature of the crack propagation depends on a number of factors including the fracture toughness' of the interface and adjoining materials, stiffness of the matrix and the particle and relative location of the crack with respect to the particles.

5 CONCLUSIONS

The predicted effective elastic and shear moduli from a 2D RVE using the EFG method for different material combinations were shown to be in good agreement with experimental and theoretical results, despite using lower nodal discretization. A modified EFG method, devoid of enrichment functions, that can capture the variable order singular stress field, predicted the SIFs to a good accuracy in FGMs. Replacing a discontinuity fibre-matrix interface with a FGM interface, was shown to be an effective alternative for making the solution scheme more robust and reducing computational effort. A case study showing two crack propagation paths in a SiC/Al composite, with a distinct interface, was also demonstrated.

Appendix A

The auxiliary displacement (u_i^{aux}), stresses (σ_{ij}^{aux}) and strains (ε_{ij}^{aux}) to determine T-stress [21] are defined by

$$\begin{aligned}
u_1^{aux} &= -\frac{E^{\#} f}{E_o \pi}\left(2\ln\frac{r}{d} + (1+v_o)\sin^2\theta\right) \\
u_2^{aux} &= -\frac{E^{\#} f}{E_o \pi}\left((1-v_o)\theta - (1+v_o)\sin\theta\cos\theta\right) \\
\sigma_{11}^{aux} &= -E^{\#}\frac{2f}{r\pi}\cos^3\theta \\
\sigma_{22}^{aux} &= -E^{\#}\frac{2f}{r\pi}\cos\theta\sin^2\theta \\
\sigma_{22}^{aux} &= -E^{\#}\frac{2f}{r\pi}\cos^2\theta\sin\theta
\end{aligned} \tag{A.1}$$

where f is a point force applied for auxiliary fields, d is an x_1-coordinate (usually taken as unity) of a fixed point at which radial and angular component of the displacement vanish (any fixed point on the x_1-axis) and

$$\begin{aligned}
&E^{\#} = \frac{E_o}{E_1^* + E_2^*}, E_o = E_m^* \forall \mathbf{x} \in \text{material } m \\
&v_o = v_m^* \forall \mathbf{x} \in \text{material } m \\
&v_m^* = \begin{cases} v_m & \text{plane stress} \\ \dfrac{v_m}{1-v_m} & \text{plane strain} \end{cases}
\end{aligned} \tag{A.2}$$

The auxiliary strains are obtained using

$$\varepsilon_{ij}^{aux} = S_{ijkl}(\mathbf{x})\sigma_{kl}^{aux} \tag{A.3}$$

where $S_{ijkl}(\mathbf{x})$ is the compliance matrix at the point $\mathbf{x}$.

REFERENCES

[1] Nicolas Moës, John Dolbow, Ted, Belytschko, "A finite element for crack growth without remeshing" *International Journal of Numerical Methods in Engineering* 1999; **46**:1103-1118.

[2] S. Mohammadi, "XFEM fracture analysis of composites", Chichester : John Wiley and Sons, 2012. - 1st Edition.

[3] Guiamatsia I., Falzon, B.G., Davies, G.A.O., Iannucci, L. "Element-free Galerkin modelling of composite damage" *Composites Science and Technology*., 2009, **69**:2640:2648.

[4] Zhen Zhang, Zhigang Suo "Split singularities and the competition between crack penetration and debond at a bimaterial interface" *International Journal of Solids and Structures* 2007; **44:**4559-4573.

[5] N. Moës, M. Cloirec, P. Cartraud, J.-F, Remacle, "A computational approach to handle complex microstructure geometries" *Computer Methods in Applied Mechanics and Engineering*, 2003; **192**:3163-3177.

[6] J. Aboudi, *Mechanics of Composite Materials, A Unified Micromechanical Approach.* Elsevier Science Publishers, Amsterdam, 1991.

[7] Z. Xia, Y. Zhang, F. Ellyin, "A unified periodical boundary conditions for representative volume elements of composites and applications" *International Journal of Solids and Structures* 2003; **40**:1907–1921.

[8] S. Kurukuri, "*A comprehensive study: Boundary conditions for representative volume elements (RVE) of composites*" Institute of Structural Mechanics. p. 13.

[9] J.F. Yau, S.S. Wang, H.T. Corten, "A mixed-mode crack analysis of isotropic solids using conservation laws of elasticity" *Journal of Applied Mechanics,* 1980; **47**:335-341.

[10] Leslie Banks-Sills, Orly Dolev, "The conservative M-integral for thermal-elastic problems" *International Journal of Fracture,* 2004; **125**:1149-1170.

[11] Hongjun Yu, Linzhi Wu, Hui Li, "T-stress evaluations of an interface crack in the materials with complex interfaces" *International Journal of Fracture,* 2012; **177**:25-37.

[12] Ki Ju Kang, "Criteria for kinking out of interface crack" *Engineering Fracture Mechanics*, 1994; **49**:587-598.

[13] M.Y. He and J.W. Hutchinson, "Kinking of a crack out of an interface" *Journal of Applied Mechanics*, 1989; **56**:270-278.

[14] R. Yuuki and J.Q. Xu, "Stress based criterion for an interface crack kinking out of the interface in dissimilar materials" *Engineering Fracture Mechanics*, 1992; **41**:635-644.

[15] A.R. Akisanya and N.A. Fleck, "Analysis of a wavy crack in sandwich specimens" *International Journal of Fracture,* 1992; **55*:***29-45.

[16] SK Maiti, RA Smith "Comparison of the criteria for mixed mode brittle fracture based on the preinstability stress-strain field Part I: Slit and elliptical cracks under uniaxial tensile loading" *International Journal of Fracture*,1983; **23**:281-295.

[17] Zvi Hashin, B. Walter Rosen "The elastic moduli of fiber-reinforce materials" *Journal of Applied Mechanics.* 1964; **11**:223-232.

[18] Hui-Zu Shari & Tsu-Wei Chou "Transverse elastic moduli of unidirectional fiber composites with fiber/matrix interfacial debonding" *Composites Science and Technology* 1995; 53:383-391.

[19] S Santhosh Kumar, V Seshu Bai, K V Rajkumar, G K Sharma,T Jayakumarand T Rajasekharan "Elastic modulus of Al–Si/SiC metal matrix composites as a function of volume fraction" in *Journal of Phyics D: Applied Physics* 2009; **42**:175504.

[20] Muthu N, Maiti SK, Falzon BG, Guiamatsia I."Computation of stress intensity factors in functionally graded materials using partition-of-unity meshfreemethod" in *Aeronaut J*, 2012; **116**:1253-1277.

[21] J. Sladek, V. Sladek, "Evaluations of the *T*-stress for interface cracks by the boundary element method" *Engineering Fracture Mechanics*, 1997; **56**:813-825.